Monolithically Integrated 100 GHz DFB-TWEAM

Marek Chaciński, Urban Westergren, Björn Stoltz, Lars Thylén, *Member, IEEE*, Richard Schatz, and Stefan Hammerfeldt

***Abstract*—A monolithically integrated distributed feedback (DFB) laser and traveling-wave electro-absorption modulator (TWEAM) with $\geq$100 GHz -3 dBe bandwidth suitable for Non-return-to-zero (NRZ) operation with on-off keying (OOK) is presented. The steady-state, small-signal modulation response, microwave reflection, chirp characteristic, and both data operation and transmission were investigated. The DFB-TWEAM was found to be an attractive candidate for future short distance communication in high bitrates systems.**

***Index Terms*—High-speed modulator, integrated device, optoelectronics, waveguide modulator.**

I. Introduction

THE monolithically integrated electroabsorption (EA) modulator with a distributed feedback (DFB) laser has become the most common high-speed transmitter in optical networks. The compact size, excellent performance and nowadays a reasonable cost were achieved due to a long time of outstanding research. This monolithical integration was crucial to combine advantages of continuous wave (CW) light from a laser with modulation property offered by external modulator. It was a breakthrough in externally modulated lasers (EML) for 10 Gb/s and 40 Gb/s [1]–[4] transmitter and it is forecasted to reach a bandwidth suitable for 100 Gb/s [5] and recently reported in [6]. In order to reach -3 dBe bandwidth of $\sim$100 GHz with sufficiently low electrical reflection, the traveling-wave electroabsorption modulators (TWEAM) were proposed [4]–[7] and demonstrated with a recently shown record low 2 V peak-to-peak (Vpp) driving voltage for 10 dB optical extinction for 230 μm total active length [8] and 2.5 Vpp for 180 μm length with improved impedance matching [9]. The segmented structures were used to overcome the limit of RC constant of long modulator. It is based on transformation of the relatively low characteristic impedance of active segments suitable for high speeds into a higher input impedance which allowed us to achieve very low electrical reflections throughout the bandwidth. These devices have been demonstrated to be useful in electrical time-division multiplexed (ETDM) transmitters with on-off-keying (OOK) up to 80 Gb/s [7]. The bitrate has been predicted to be extendable to 100 Gb/s which is the goal of ongoing development for 100 Gb/s Ethernet transmission [5]. The progress on work related to other 100 Gb/s components such as multiplexer (MUX), driver amplifier (TWA), receiver, clock and data recovery circuit (CDR), and demultiplexer (DeMUX) are reported elsewhere is indicated in [5].

This work presents more complete properties and details of design and performance of the 100 GHz monolithically integrated DFB-TWEAM device The paper is divided into the following parts. The integration, fabrication, and design are presented. Then the investigation of the steady state performance of the laser and both the steady state and modulation properties of the modulator are covered by the next section. The paper is closed by conclusions and future work sections.

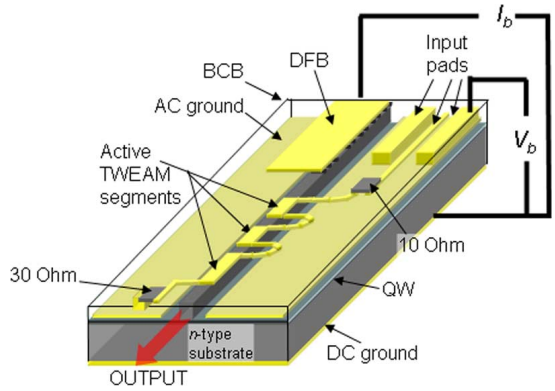

Fig. 1. Schema of DFB integrated with non-periodic 3-segment TWEAM and the biases connections.

II. Design and Device

The DFB-TWEAM and biasing schema are illustrated in Fig. 1. The quantum wells (QW) were optimized separately for the DFB laser and the EA modulator. Different designs and number of wells were necessary to make a trade-off between high gain for the laser material and high absorption in the quantum confined Stark effect (QCSE) for the modulator. Both gain and modulator materials were grown by metal vapour phase epitaxy (MOVPE) using a constant flow of hydrides, as described in [10]. The gain section consisted of 7 QWs 7 nm thick, whereas the modulator had 12 QWs of 9 nm thickness. These were integrated using a butt-joint technique. The grating for the DFB-section was defined by e-beam lithography. After the final cladding and contact re-growth the components were formed in standard ridge waveguide structures. The formation of ac-ground, BCB, electrodes, NiCr resistor, was similar to

Manuscript received September 29, 2008; revised December 17, 2008. First published April 24, 2009; current version published July 24, 2009.

M. Chaciński, U. Westergren, and R. Schatz are with the Kista Photonic Research Centre (KPRC), Royal Institute of Technology KTH, Electrum 229, 164 40 Kista, Stockholm, Sweden (e-mail: marekch@kth.se; urban@kth.se; thylen@kth.se; rschatz@kth.se).

B. Stoltz and S. Hammerfeldt are with Syntune AB, 164 40 Kista, Sweden (e-mail: bjorn.stoltz@syntune.com; stefan.hammerfeldt@syntune.com).

L. Thylén is with the Kista Photonic Research Centre (KPRC), Royal Institute of Technology KTH, Electrum 229, 164 40 Kista, Stockholm, Sweden and also with Hewlett-Packard Laboratories, Palo Alto, CA 94304 USA (e-mail: lthylen@kth.se).

Color versions of one or more of the figures in this paper are available online at http://ieeexplore.ieee.org.

Digital Object Identifier 10.1109/JLT.2009.2015773

the components reported in [6]. The electrodes for DFB and EA contacts were made in a single process run. The active modulator segments were defined by the metal electrode structure and optimized p-doping instead of diffusion, as published earlier [6]. The doping level and thickness were carefully designed to obtain resistance sufficiently low to provide charges to/from electrodes and active sections, and at the same time high enough to avoid current flow between the sections along the mesa. An additional etching of the InGaAs contact layer between sections was introduced to achieve even higher electrical isolation (typically isolation along the mesa is on order of kOhm/μm, resulting in >50 kOhm resistance between DFB and first TWEAM electrode, and >10 kOhm between segments). In order to eliminate potential crosstalk to the DFB, the input signal electrode to the modulator is shielded from the laser by vertical plating through the BCB from the input pad ground electrodes to the ac ground.

As mentioned the QWs composition for DFB was already chosen and other parameters such as length, strength of grating, phase shift were specially designed. The laser was 440 μm long with a grating designed to have most of the output power towards the EA side. The RT photoluminescence peak was at 1.55μm. The wafer was cleaved into bars and then anti-reflective coated on the output side. The lasers were made at three different wavelength: 1.53; 1.54; 1.55 μm by varying the grating period and keeping same 50% duty cycle.

The design of the EA was based on earlier QW designs. The PL peak was around 1.48 μm as in [6]. The optimization was mostly on the electrode part and segmentation. It took into account a few aspects, namely the return loss (electrical reflection, S_{11}), the optoelectrical bandwidth (S_{21}), and modulation efficiency. TWEAM structures were designed with non-periodic segmentation. However modulators with 2- and 3-active segments were similar in layout to [8] and [9], respectively, but this work highlights other aspects and hence a 3-segment device was selected for investigations. A 30 Ohm on-chip termination resistor was used to achieve the necessary low reflection for the signal. A 10 Ohm on-chip series resistance at the input was introduced in selected 3-segments components to have >40 Ohm (together with the metal electrode on top) input resistance at low frequencies [9], which give rise to slightly higher drive voltage. The total active length of a 3-segments EA was 180 μm (230μm for 2-segments), divided between the lengths of 40, 40 and 100 μm (70 and 160 μm for 2-segments), with the shorter segments closest to the input pad. A periodic structure with two or more segments will have a degenerate resonance due to the active low-impedance segments and higher-impedance transmission lines, while a non-periodic structure provides an extra degree of freedom in the design which can be used to increase either the bandwidth or the total active length. In a non-periodic structure, the resonances can be separated and used to tune the transfer function for increased bandwidth with a flat response while the return loss can be kept relatively low throughout the bandwidth (see, e.g., [8, Ref. [4]]). This increased bandwidth can then be used to increase the length to improve efficiency.

In principle the active length in the 3-segments structure can be longer, which will reduce driving voltage, but due to fabrication simplicity the total size of the modulator was fixed and

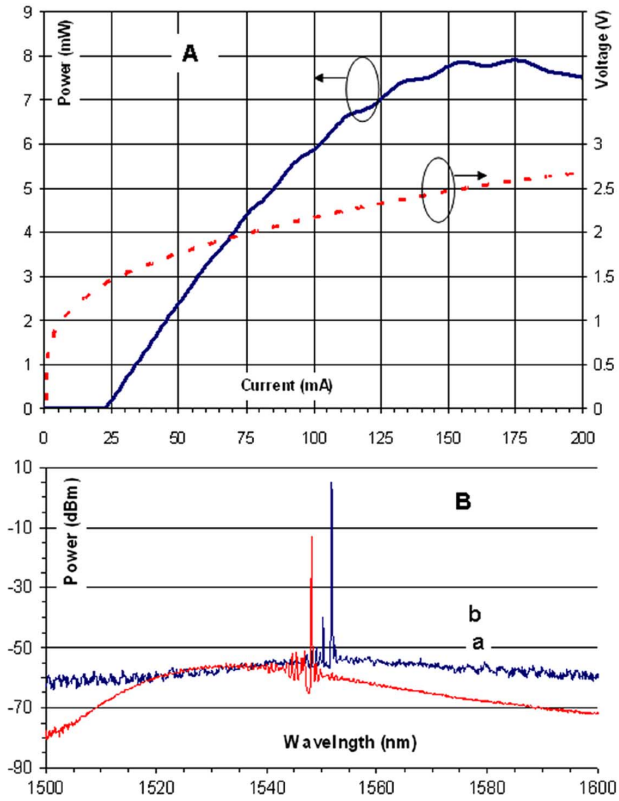

Fig. 2. (A) Light (solid line) and voltage (dashed line) versus bias current characteristic of typical DFB monolithically integrated with TWEAM. Curves measured at RT with non-biased modulator from EA facet. (B) optical spectra at I_b equal (a) 25 mA and (b) 150 mA.

the electrical isolation between segments required some space. The size of the input pads was increased (compared to [7]) and formed as a taper (not shown) to decrease effective pad fringing capacitance and allow probing, flip-chip or wire bonding for subsequent packaging [5]. The metal thickness of the top electrode was increased (to $\sim$2 μm) by electroplating to reduce the microwave loss at high frequencies and to decrease the ratio between electrode and mesa resistance. Both the DFB and the TWEAM were designed to operate with TE-polarized light. The different wavelengths of the DFBs were made in order to investigate the structures with respect to temperature and wavelength.

III. Experimental Setup and Measurements Results

The DFB-TWEAM bars were placed on a thermistor-equipped heat sink, where the operating temperature was stabilized. The steady-state performances were measured with a large area detector (Agilent 81618A), and the modulation responses were tested with output light coupled into a singlemode fiber (SMF), with a home made lensed fiber at room temperature (RT). The optical spectra were measured and recorded with an optical spectrum analyzer (OSA, Agilent 86140B). The typical light-current-voltage (LIV) characteristic of laser operated at RT with unbiased EA is shown in Fig. 2(A) (output of EA side), where the optical spectra of laser biased at 25 and 150 mA, which is slightly above threshold and at maximum power $(P_{\max})$ before rollover occurs [see Fig. 2(B)].

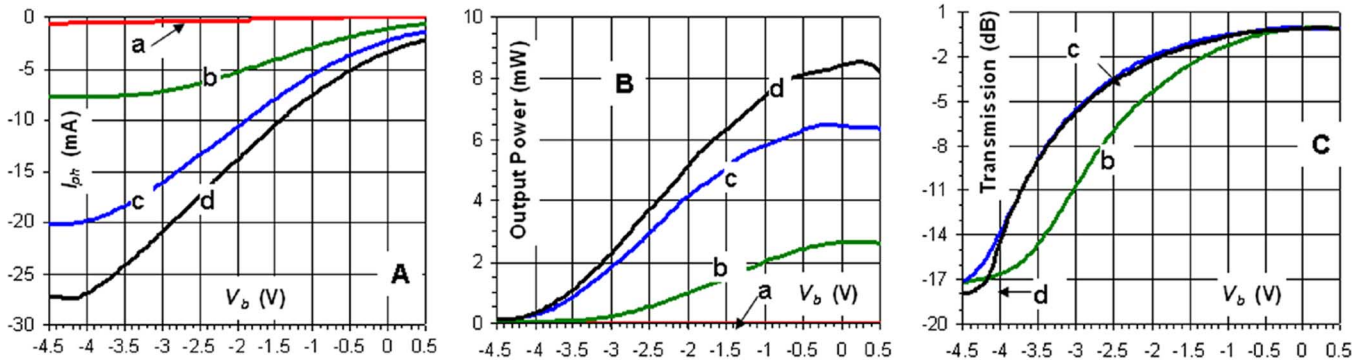

Fig. 3. Room temperature (RT) steady-state performance on EA: (A) absorption photo-current $(I_{\rm ph})$, (B) optical output power, (C) normalized transmission versus bias voltage (V_b) with CW input light from integrated DFB laser. Curves a-d correspond to DFB bias currents (I_b) 0; 50; 100 and 150 mA.

The DFB-laser exhibited a threshold current $I_{\rm th}$ of 23 mA and a side-mode-suppression-ratio (SMSR) of about 45 dB at $P_{\rm max}$ (see Fig. 2). The observed wavelength shifts were 0.02 and 0.03 nm/mA for low and high bias currents (I_b), respectively. The output slope on the EA side was 8 mW/A, and with assumed value of waveguide loss of the EA (6 dB/mm) and the low light from the rear facet it was possible to estimate differential-quantum-efficiency of the laser (of $>$20%). The maximum output from the chip was $\sim$9 mW ($\sim$18 mW into EA) and the laser was operating in singlemode over the entire bias range [from $I_{\rm th}$ to rollover, see Fig. 2(B)]. No mode hop occurred when varying bias current. The resistance was 7 Ohm.

Steady-state transmission and current versus voltage (I-V) characteristics of modulator are presented in Fig. 3(A)–(C). The EA exhibited dark current (I_D) of 0.47 mA (at RT, and 4 V reverse biased V_b) and is able to operate at $P_{\rm max}$ of the DFB resulting in absorption photo current $(I_{\rm ph})$ >27 mA (at RT and $V_b = 4$ V). The EA exhibited approximately linear characteristic of $I_{\rm ph}$ versus input power (not shown), also at constant optical input. The relation between V_b and $I_{\rm ph}$ was similar until it reaches the point where light was completely absorbed. The normalized steady-state extinction is estimated to be about 15 dB for 2 V voltage change. A deep analysis of internal heating caused by the bias current (I_b) of the DFB and $I_{\rm ph}$ of the modulator, other thermal properties of both parts of the component and wavelength dependence of material parameters (gain and absorption) are left for further study.

In the high speed tests the modulator was electrically connected (see Fig. 1) by a high-frequency 75 μm pitch ground-signal-ground (GSG) probe attached to the input pads and via the substrate, where the bias current to the DFB was fed by dc-probe and substrate. Reverse dc bias was supplied to the TWEAM via the ac ground (connected to the GSG probe) and the substrate. The (CW) input light into the modulator was provided by the integrated laser and the optical output was coupled to the measurement equipment with a home made lensed fiber. The small signal modulation responses (electrical reflection S_{11} and electro-optical S_{21}) were measured with an incident electrical signal power of -10 dBm from a Precision Network Analyzer (PNA, Agilent E8361A). The EA was tested at RT with various conditions of the optical power (varying I_b between 0 and 150 mA) and bias voltage (V_b in range of -0.8 to -4 V). As mentioned the S_{11}, and the S_{21} were measured up to 70 GHz.

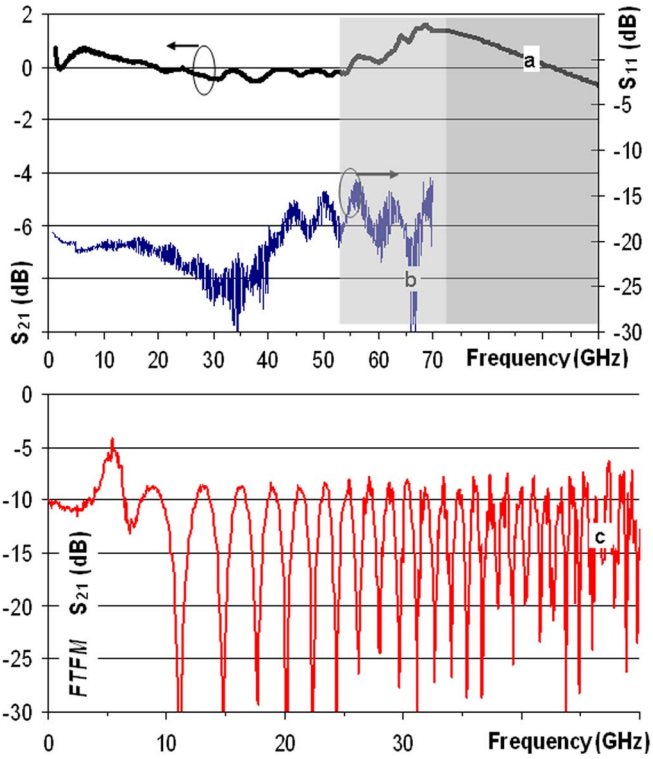

Fig. 4. Measured and extrapolated small-signal transfer characteristics (S_{21}) and electrical reflection (S_{11}) of TWEAM (on the top). The curves for S_{21} show response of TWEAM without PD and with extrapolation (a). The (b) and (c) curves show S_{11} and chirp (on the bottom, actual response scale is modified by fiber loss and EDFA gain and frequency limited to enhance visibility) measurements, respectively. The region of uncertain PD response is indicated by gray field, where the modeled response is in dark gray. Curves correspond to measurements carried under 1.6 V (curves a, b) and 3 V (curve c) biases of TWEAM, respectively, and DFB operating at 70 mA bias current.

For the optoelectrical conversion we used a commercial 50 GHz bandwidth photodiode (PD, u2t-XPD2020R) and a 6 dB/octave roll-off was assumed at higher frequencies. The S_{21} of the TWEAM was achieved by subtraction of PD response. The typical responses of the S_{11} and the resulting S_{21} of the modulator are shown on Fig. 4. The characteristic was flat from

low frequencies to 70 GHz within the estimated accuracy of the measurement setup ($< \pm 1$ dB) with a slight peak in the upper part of the frequency range. We observed that the response level is related to bias conditions, which could be concluded from dc measurements, but there was no difference in the -3 dBe bandwidth. A circuit simulation model for the TWEAM [6], [8] was used to estimate the roll-off of the TWEAM from 70 to 100 GHz to about 2 dB. We concluded that the -3 dBe bandwidth was $\geq$100 GHz for the TWEAM, which makes this result consistent with [6]–[9]. The measured (at $I_b = 50$ mA) S_{11} was lower than -13 dB up to 70 GHz, which indicates that the 3-segments design with an extra series resistance provides better matching to 50 Ohm systems with the expense of a small increase in the drive voltage due to the voltage division at the input (see Fig. 4 curve b). A small increase in reflection loss (compared to dark current measurements) was attributed to induced resistance, due to absorption of the light in EA. The small signal chirp characteristic was performed in fiber-transfer-function-method (FTFM) [11] with a 82 km long SMF used as the frequency discriminator. The measured response curve is exhibited in Fig. 4 (curve c) and the minima of the response were used to extract the chirp factor (α_H, called α-factor). With the biases conditions $I_b = 70$ mA; $V_b = 3$ V the $\alpha_{\rm H}\sim$0.3 has been obtained. The measured response is limited to 50 GHz due to a drop of signal to noise ratio caused by signal attenuation in the fiber. The scale is modified to increase visibility of all curves. The dispersion length product of the fiber and the first minima resonance indicated that transmission of non return to zero (NRZ) on-off keying (OOK) 100 Gb/s signal will be dispersion limited to 500 m long SMF cable.

Large signal modulation was measured at the same bias conditions. The 2 Vpp output modulation signal composed of pseudo random bit sequences (PRBS,) of word length 2^7-1 was achieved by time domain multiplexing (TDM) of four 12.5 Gb/s PRBS data streams. A 4:1 multiplexer (MUX, SHF5005) and pulse-pattern-generator (PPG, Anritsu MP1758A) were used to generate NRZ 50 Gb/s true PRBS signal. It can be deduced from Fig. 3(C) and it was already pointed out in the note of the response that the modulation level depends on the bias conditions. Hence the extinction ratio (ER) for a given driving voltage Vpp can be influenced by V_b.

Higher V_b results in larger slope dB/V but it decreases also the average output power [see Fig. 3(B)–(C)]. Thus compromise can be achieved with adjustment of the operating conditions. The wavelength dependence as well as mentioned thermal impact will be investigated in the future. The 50 Gb/s eye diagrams for transmission over 0 km and 2.2 km long SMF are presented in Fig. 5(A)–(B). The frequency dependent loss of a 0.5 m long coax cable, the PD and 44 GHz bandwidth of the electrical port of digital sampling oscilloscope (DSO, Agilent 86100B) contributed to the overall bandwidth limit of the setup, but the eyes were open indicating that the DFB-TWEAM has flat response under large signal operation for frequencies up to $\sim$50 GHz. The estimated modulation input signal at the pads of the device was lower than 1.8 Vpp (1.6 Vpp at 35 GHz) with a MUX output of 2 Vpp and $\sim$1 dB (2 dB at 35 GHz) cable loss. 4 dB ER in the receiver was achieved at the chosen V_b as a compromise to reach an average output power (with 1 dB modulator optical loss) which was high enough for the measurement system sensitivity. The received ER was reduced by the limited bandwidth of the receiver system, and the expected ER for the modulator is $\sim$8 dB at the transmitter output for 2 Vpp modulation signal at the pads. Noise contribution to the transmission over 2.2 km was observed.

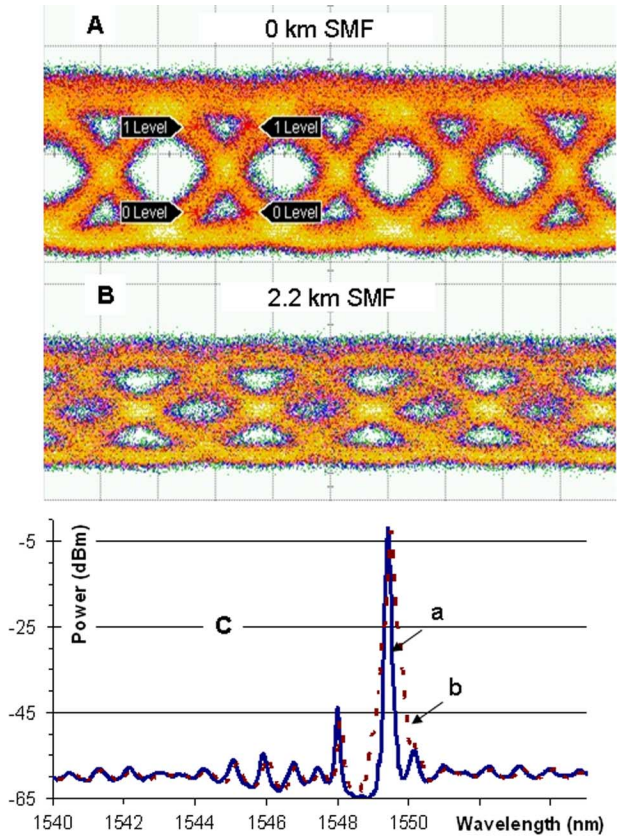

Fig. 5. Data operation under $<$1.8 Vpp modulation input signal with transmission over (A) 0 km and (B) 2.2 km long SMF. The achieved extinction ratio was 4 dB for 0 km. Scales are 10 ps/div and 3 mV/div. (C) OSA recorded spectra (a) without modulation and (b) under modulation.

The optical spectra with and without modulation input signal are shown in Fig. 5(C). With inserted modulation signal a slight broadening of the spectra was observed. It should be pointed out that the data operation and transmission were performed without use of optical amplifiers and filters. This was possible due to sufficiently high output light delivered from the EA facet of the integrated device. Transmission trial has been implemented to investigate a cost effective solution of high bitrates and direct connections in a short distance of an optical network for possible future 100 GbE. By scaling of the bitrates and observation of eyes after transmission over 2.2 km long fiber we estimated that it should be possible to use $\sim$500 m long SMF cable to send 100 Gb/s data streams with NRZ OOK modulation format.

IV. Conclusion and Further Work

A high speed traveling-wave EA modulator monolithically integrated with DFB laser was demonstrated. The devices were fabricated with active segments defined only by electrode layout and epitaxial growth of Zn-doped layer has been introduced to

control the thickness of intrinsic layer and merge of laser and modulator materials. The small-signal response measurements and extrapolation resulted in modulation -3 dBe bandwidth beyond 100 GHz. The electrical reflection loss is lower than 13 dB over the measured 70 GHz frequency range. The TWEAM exhibited steady-state extinction ratio of >15 dB for 2 V voltage change with laser operating at maximum power. The large bandwidth combined with high output power and high modulation efficiency makes the device an attractive candidate for next generation 100 Gb/s Ethernet. The same properties indicate that the DFB-TWEAM can be a cost effective solution with a dispersion limited distance of about 500 m in SMF for 100 Gb/s data rates with NRZ OOK modulation. In similar manner as in previous work [12] EA operation as detector will be investigated. It is expected that new and better controlled epitaxial layers will provide a higher detection bandwidth due to shorter transit time of the photo-generated carriers.

ACKNOWLEDGMENT

The design and measurements were carried out with partial financial support by the European Commission via the IST FP6 project HECTO [5]. The high-speed instruments were funded in part by the Knut & Alice Wallenberg foundation, (KAW).

REFERENCES

[1] H. Fukano, T. Yamanaka, M. Tamura, and Y. Kondo, "Very-low-driving-voltage electroabsorption modulators operating at 40 Gb/s," *IEEE/OSA J. Lightw. Technol.*, vol. 24, pp. 2219–2224, May 2006.

[2] J.-W. Shi, A.-C. Shiao, C.-C. Chu, and Y.-S. Wu, "Dual-depletion-region electro-absorption modulator with evanescently-coupled waveguide wavelength for high-speed (>40 GHz) and low driving-voltage performance," *Photon. Technol. Lett.*, vol. 19, pp. 345–347, Mar. 2007.

[3] Y. Luo *et al.*, "40 GHz AlGaInAs multiple-quantum-well integrated electroabsorption modulator/distributed feedback laser based on identical epitaxial layer scheme," *Jpn. J. Appl. Phys.*, vol. 45, no. 40, pp. L1071–L1073, 2006.

[4] L. Thylén, U. Westergren, P. Holmström, and P. Jänes, "Chapter 7 in 5th Edition of Optical Fiber Telecommunications VA: Components and Subsystems," in *Recent Developments in High Speed Optical Modulators*. Amsterdam, The Netherlands: Elsevier, 2008, (ISBN 978-0-12-374171-4).

[5] [Online]. Available: www.hecto.eu

[6] R. Lewén, S. Irmscher, U. Westergren, L. Thylén, and U. Eriksson, "Segmented transmission-line electroabsorption modulators," *JLT*, vol. 22, no. 1, pp. 172–179, Jan. 2004.

[7] Y. Yu, R. Lewén, S. Irmscher, U. Westergren, L. Thylén, U. Eriksson, and W. S. Lee, "80 Gb/s ETDM transmitter with a traveling-wave electroabsorption modulator," presented at the OFC 2005 OWE1, Anaheim, CA, 2005.

[8] M. Chaciński, U. Westergren, B. Willén, B. Stoltz, and L. Thylén, "Electroabsorption modulators suitable for 100-Gb/s ethernet," *EDL*, vol. 29, no. 9, pp. 1014–1016, Sep. 2008.

[9] M. Chaciński, U. Westergren, B. Stoltz, and L. Thylén, "Monolithically integrated DFB-EA for 100 Gb/s ethernet," *EDL*, vol. 29, no. 12, pp. 1312–1314, Dec. 2008.

[10] A. Mircea, A. Ougazzaden, G. Primot, and C. Kazmierski, "Highly thermally stable, high-performance InGaAsP:InGaAsP MQW structures for optical devices by atmospheric pressure MOVPE," *J. Crystal Growth*, vol. 124, pp. 737–740, 1992.

[11] F. Devaux, Y. Sorel, and J. F. Kerdiles, "Simple measurement of fiber dispersion and of chirp parameter of intensity modulated light emitter," *J. Lightw. Technol.*, vol. 11, no. 12, pp. 1937–1940, Dec. 1993.

[12] M. Chaciński, U. Westergren, L. Thylén, R. Schatz, and B. Stoltz, "50 Gb/s modulation and/or detection with a traveling-wave electro-absorption transceiver," in *OFC 2008*, San Diego, CA, vol. JThA32.

Marek Chaciński received the M.Sc. degree in optoelectronics and fibreoptical communication from the Wroclaw University of Technology (WUT), Poland, in 2002.

From 2001 to 2002, he worked as a Research Engineer in Institute for Microelectronics Mainz, Germany. In 2002, he joined the Laboratory of Photonics and Microwave Engineering at KTH as a Ph.D. student. He has been teaching microwave engineering and fibreoptical communication in undergraduate courses at KTH since 2003. He has supervised and provided help for over five M.Sc. theses. He has worked in cooperation with other KTH departments, universities and companies such as PhoXtal, Zarlink, Optillion, Northlight, Svedice, Acreo and Syntune conducting expertise and components evaluation in electronics and photonics. He has been an active member of COST 288. He has been working for more than five European and national projects, and two Networks of Excellence. He is deputy of the Photonic Systems Measurement Laboratory at KTH, which is part of the Kista Photonics Research Center (KPRC) where provide measurements such as network analysis up to 70 GHz and bit-error rate testing up to 60 Gb/s and conducting transmission experiments. He is interested in design and measurement of transmitters and receivers for various types of fiberoptical communication. The research has mainly focused on directly modulated semiconductor lasers i.e., long wavelength VCSELs and edge emitting lasers for speeds of 10 and 40 Gb/s aiming in short distance application and modulators Mach-Zehnder type and electroabsorption for use in transmitters for long hole communication. During the last years the research has focused on state-of-the-art electroabsorption modulators for use in transmitters for speeds from 100 to 160 Gb/s.

Urban Westergren received the M.Sc. degree in engineering physics in 1984, the Ph.D. in electrical engineering 1992, and the Docent degree in photonics and microwave engineering in 2002, all from the Royal Institute of Technology (KTH), Stockholm, Sweden.

From 1984 to 1993, he worked as a Research Engineer in high-speed electronics at the Swedish Institute of Microelectronics (IM), Kista, Sweden. In 1994, he joined the Laboratory of Photonics and Microwave Engineering, KTH as a Research Associate and in 1996 he was appointed to his current position of Associate Professor. From 2000 to 2003, he was Senior Expert in electronic design at Optillion AB. He has been teaching microwave engineering and high-speed electronics in various graduate and undergraduate courses at KTH since 1984. He has been the teacher and examiner of several hundreds of undergraduate students and over a 100 graduate students in these courses. He has supervised or examined over 20 M.Sc. theses, and he has been a member of 15 Ph.D. evaluation boards and two Docent evaluation boards, and he is the Program Director for the Master's programme in Photonics at KTH. He was the main applicant to the Euroepan Commission for a Specific Targeted Research Project in 2005, and he is the Coordinator of the resulting project HECTO (www.hecto.eu) since 2006. He manages the Photonic Systems Measurement Laboratory at KTH, which is part of the Kista Photonics Research Center (KPRC) and currently includes equipment for, e.g., network analysis to 60 GHz and bit-error rate testing to 50 Gb/s. His research at KTH has included design and measurement of receivers and transmitters for fiberoptical communication at very high bitrates. During the last years the research has focused on state-of-the-art electroabsorption modulators for use in transmitters for speeds from 100 to 160 Gb/s.

Björn Stoltz, photograph and biography not available at the time of publication.

Lars Thylén (M'91) received the M.Sc. degree in electrical engineering and the Ph.D. degree in applied physics both from the Royal Institute of Technology (KTH), Stockholm, Sweden, in 1972 and 1982, respectively.

From 1973 to 1982 he was with SRA Communications, working in the areas of image processing, diffraction optics and optical signal processing. From 1976 to 1982, he held a research position at the Institute of Optical Research, Stockholm, where he was engaged in research in integrated and guided wave optics, notably waveguide theory, RF spectrum analysis, and optical signal processing. In 1982, he joined Ericsson, heading a group doing research in the areas of integrated photonics in lithium niobate and in semiconductors and its applications to optical communications and switching. From 1985 to 1986, and in 2007, he was a Visiting Scientist with the Department of Electrical Engineering and Computer Sciences, University of California, Berkeley, and in spring 2008 and 2009 at HP Laboratories, Palo Alto, CA. He has also been a Visiting Scientist with the Optical Sciences Center at the University of Arizona, Tucson and in fall 2001, at the University of California at Santa Barbara, working on applications of quantum optics. In 1987, he was appointed Adjoint Professor at the Department of Microwave Engineering, Royal Institute of Technology, Stockholm. He was active in the inception, planning and running of the EU RACE I OSCAR project as well the pioneering RACE II MWTN (Multiwavelength transport network) project and ACTS METON project, and has given a number of invited papers on these projects. Since 1992, he is a Professor at the Department of Microelectronics and Applied Physics, KTH, heading the Laboratory of Photonics and Microwave Engineering. From 1992 to 1997, he was a consultant to Ericsson. From 1999 to 2002, he was Program Director of the Swedish Photonics Research program, supported by the Swedish Foundation for Strategic Research, and comprising KTH and Chalmers University photonics research. From 2003 to 2007, he was Director of the Strategic Research Center in Photonics at KTH, funded by the Swedish Foundation for Strategic Research. He was active in the inception and planning of the Kista Photonics Research Center, implementing a coordinated photonics research effort in the Stockholm area. He is also one of two Chief Scientists of the Joint Research Center of Photonics of the Royal Institute of Technology and Zhejiang University (China), founded in 2003. He was a co-founder of Optillion AB, a startup in the area of 10 Gb/s+ Ethernet transceivers, and is a co-founder and board member of PhoXtal Communications AB, a transceiver company. He is CEO of a Chinese start up, Fuyang Photonics in Fuyang city, a consulting company. Current research interests include nanophotonics, high density integrated photonics, devices for photonic switching and high speed modulation, quantum optics as well as the physics involved in electronic and photonic switching operations. He has authored or coauthored more than 200 journal papers and conference contributions as well as several book chapters and has been granted approximately 20 patents.

Prof Thylén is a member of the Optical Society of America as well as a member of the Royal Swedish Academy of Engineering Sciences. He has served on program committees for major optics conferences such as European Conference on Optical Communications, ECOC, and Optical Fiber Communications, OFC, and on a large number of OSA and IEEE conferences. He has further served as Program Chair and General Chair for the 1995 and 1997 OSA Topical Meetings on Photonics in Switching, respectively. He was General Cochair and Technical Program Committee Chair of ECOC 2004 in Stockholm and General Chair for the 2008 Asia Pacific Optical Communications Conference in China.

Richard Schatz was born in 1963. He received the Ph.D. degree in photonics from the Royal Institute of Technology (KTH), Stockholm, Sweden, in 1995.

Since 1987, he has conducted research in the field of semiconductor lasers at the Laboratory of Photonics and Microwave Engineering, KTH). He spent 1992 as a Visiting Scientist at AT&T Bell Laboratories, Murray Hill, NJ. His research is mainly focused on modeling and dynamic characterization of photonic components, both edge emitter lasers, VCSELs and modulators and he has authored or coauthored more than 100 journal papers and conference contributions. Special areas of interest are spatial hole burning effects in DFB lasers, detuned loading effects in DBR lasers and Roman and Greek coins.

Stefan Hammerfeldt, photograph and biography not available at the time of publication.